18th International Conference
ENGINEERING MECHANICS 2012
Svratka, Czech Republic, May 14 – 17, 2012

pp. 363–375
Paper #175

OPTIMAL SEMI-ACTIVE PREVIEW CONTROL OF A QUARTER CAR MODEL WITH MAGNETORHEOLOGICAL DAMPER WITH RESPECT TO TIRE LIFT OFF

F. Havelka[*], M. Musil[**]

Abstract: *A quarter car model with magnetorheological (MR) damper is studied. An adopted experimentally verified non – linear hysteretic mathematical model is used to represent the MR damper. Approaching road disturbances are measured by a sensor. Optimal preview control strategy for fully active suspension is derived with respect to road holding, suspension rattle space and ride comfort. Continuous inverse mathematical model of the MR damper for the use of control is derived such that force generated by MR damper matches the control force of fully active system if possible. In the simulations, the effect of tire lift off is modeled using a continuous mathematical function.*

Keywords: ***quarter car, MR damper, optimal preview control, tire lift off***

1. Introduction

In recent years active and semi-active suspensions have been investigated due to their ability to adapt to various types of road excitations. Compared with passive suspension systems, which can only dissipate the energy present in the system, active suspension systems can supply the flow of energy into the system and can generate forces which are independent of the state of the system. Effective compromise between passive and active suspension systems are semi-active suspensions. Semi-active suspension systems are less expensive than the active ones, they require much less energy intensive source and even if the source of energy fails they can still operate as passive suspension systems.

In this paper a magnetorheological damper is utilized in the suspension system as a semi-active part. An experimentally verified non-linear hysteretic mathematical model is used to represent the dynamics of the MR damper. A basic quarter car model is utilized to simulate the vertical dynamics of vehicle. For the use of control algorithm a continuous inverse mathematical model of the MR damper is derived. Dissipative force generated by the MR damper tries to match the one generated by a fictive ideal active system. Optimal preview control strategy for the fully active system with respect to road holding, suspension rattle space and ride comfort is derived such that it is supposed that approaching road disturbances are measured by a sensor and are known within a certain distance ahead. Active and semi-active suspension systems with preview are examined in vehicle travelling over a bump and in both cases the effect of tire lift off is investigated.

2. Quarter car model with idealized active suspension and with consideration the tire lift off

To simulate the vertical dynamics of vehicle, the quarter car model is utilized – figure 1a.). The equations of motion with consideration the tire lift off problem are follows:

$$\begin{aligned} m_1\ddot{y}_1 &= -k_1\left(y_1 - y_2\right) + u - m_1 g \\ m_2\ddot{y}_2 &= -k_2\left(y_2 - w\right)\left[1 - H\left(y_2 - w\right)\right] - k_1\left(y_2 - y_1\right) - u - m_2 g \end{aligned} \tag{1}$$

where *H(-)* is the heaviside step function and *u* is the force generated by active control element, which dynamics is neglected.

[*] Ing. Ferdinand Havelka: Institute of Applied Mechanics, Faculty of Mechanical Engineering, Slovak University of Technology, Námestie slobody 17; 812 31, Bratislava 1; SK, e-mail: ferdinand.havelka@stuba.sk

[**] doc., Ing. Miloš Musil, Ph.D.: Institute of Applied Mechanics, Faculty of Mechanical Engineering, Slovak University of Technology, Námestie slobody 17; 812 31, Bratislava 1; SK, e-mail: milos.musil@stuba.sk

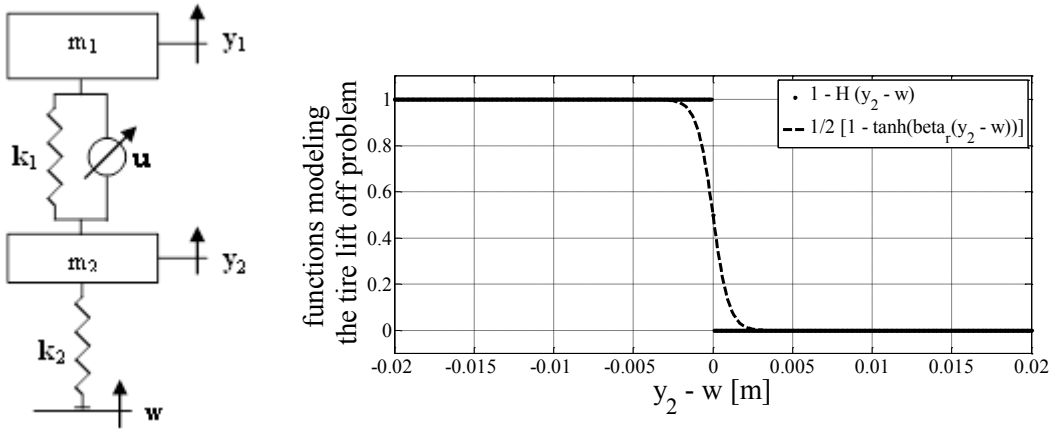

a.) *b.)*

Fig. 1: a.) quarter car model with active suspension
b.) functions modeling the tire lift off problem

The function modeling the tire lift off problem can be rewritten into form:

$$1-H\left(y_2-w\right)=\frac{1}{2}\left[1-\operatorname{sgn}\left(y_2-w\right)\right]\cong\frac{1}{2}\left\{1-\tanh\left[\beta_r\left(y_2-w\right)\right]\right\} \tag{2}$$

where now the function *tanh(-)* is a continuous function and β_r is a coefficient large enough.

Noting the relation (2), equations of motion in the matrix form are:

$$\mathbf{M_a}\ddot{\mathbf{q}}_{\mathbf{aA}}+\mathbf{K_{aL}}\mathbf{q_{aR}}+\mathbf{K_{aN}}\mathbf{q_{aR}}\mathbf{e_a}\tanh\left(\beta_r\mathbf{q_{aR}}\right)=\mathbf{b_{ag}}g+\mathbf{b_u}u \tag{3}$$

where

$$\begin{gathered}\mathbf{M_a}=\begin{bmatrix}m_1&0\\0&m_2\end{bmatrix},\ \mathbf{K_{aL}}=\begin{bmatrix}k_1&0\\-k_1&\frac{k_2}{2}\end{bmatrix},\ \mathbf{K_{aN}}=\begin{bmatrix}0&0\\0&-\frac{k_2}{2}\end{bmatrix},\ \mathbf{e_a}=\begin{bmatrix}0\\1\end{bmatrix}^T,\\ \mathbf{b_{ag}}=-\begin{bmatrix}m_1\\m_2\end{bmatrix},\ \mathbf{b_u}=\begin{bmatrix}1\\-1\end{bmatrix},\ \mathbf{q_{aA}}=\begin{bmatrix}y_1\\y_2\end{bmatrix},\ \mathbf{q_{aR}}=\begin{bmatrix}y_1-y_2\\y_1-w\end{bmatrix}\end{gathered} \tag{4}$$

Transformation from absolute to the relative coordinates is realized through the equation:

$$\mathbf{q_{aR}}=\mathbf{T_{aA}}\mathbf{q_{aA}}+\mathbf{T_{aw}}w \tag{5}$$

where

$$\mathbf{T_{aA}}=\begin{bmatrix}1&-1\\0&1\end{bmatrix},\ \mathbf{T_{aw}}=\begin{bmatrix}0\\-1\end{bmatrix} \tag{6}$$

Combining equation (3) and differentiated equation (5), state space model of system in the figure 1 a.) is obtained:

$$\dot{\mathbf{x}}_\mathbf{a}=\mathbf{A_{aL}}\mathbf{x_a}+\mathbf{A_{aN}}\mathbf{x_a}\mathbf{E_a}\tanh\left(\beta_r\mathbf{x_a}\right)+\mathbf{B_a}u+\mathbf{G_a}\mathbf{f_{gw}} \tag{7}$$

where

$$\begin{gathered}\mathbf{A_{aL}}=\begin{bmatrix}\mathbf{O_a}&\mathbf{T_{aA}}\\-\mathbf{M_a}^{-1}\mathbf{K_{aL}}&\mathbf{O_a}\end{bmatrix},\ \mathbf{A_{aN}}=\begin{bmatrix}\mathbf{O_a}&\mathbf{O_a}\\-\mathbf{M_a}^{-1}\mathbf{K_{aN}}&\mathbf{O_a}\end{bmatrix},\ \mathbf{E_a}=\begin{bmatrix}\mathbf{e_a}^T\\\mathbf{o_a}\end{bmatrix}^T,\ \mathbf{B_a}=\begin{bmatrix}\mathbf{o_a}\\\mathbf{M_a}^{-1}\mathbf{b_u}\end{bmatrix},\\ \mathbf{G_a}=\begin{bmatrix}\mathbf{G_{ag}}&\mathbf{G_{aw}}\end{bmatrix},\ \mathbf{G_{ag}}=\begin{bmatrix}\mathbf{o_a}\\\mathbf{M_a}^{-1}\mathbf{b_{ag}}\end{bmatrix},\ \mathbf{G_{aw}}=\begin{bmatrix}\mathbf{T_{aw}}\\\mathbf{o_a}\end{bmatrix},\ \mathbf{f_{gw}}=\begin{bmatrix}g\\\dot{w}\end{bmatrix},\ \mathbf{x_a}=\begin{bmatrix}\mathbf{q_{aR}}\\\dot{\mathbf{q}}_{\mathbf{aA}}\end{bmatrix}\end{gathered} \tag{8}$$

where $\mathbf{O_a}$ and $\mathbf{o_a}$ are zero matrix and vector respectively of appropriate dimensions.

3. Optimal linear preview control of idealized active suspension

Optimal linear control without preview has been widely utilized in active suspensions regulation. As was shown by many authors, e.g. (Hać & Youn, 1991; Hać, 1992; Thompson & Pearce, 1998), optimal linear control with preview, i.e. the case when approaching road disturbances are known within a certain distance ahead, reduces variances of car body acceleration, suspension travel and tire deflection at the same time compared with the no preview case.

In this section, optimal linear preview control of idealized active suspension is derived. Incoming road disturbances are measured by a sensor at some distance ahead of the vehicle. The tire lift off effect is not considered in the deriving. The equations of motion for such a problem are:

$$\mathbf{M_a}\ddot{\mathbf{q}}_{\mathbf{aA}} + \mathbf{K_a}\mathbf{q}_{\mathbf{aR}} = \mathbf{b_u}u \tag{9}$$

where

$$\mathbf{K_a} = \begin{bmatrix} k_1 & 0 \\ -k_1 & k_2 \end{bmatrix} \tag{10}$$

The remaining variables are described above. Combining equation (9) and differentiated equation (5), state space model of idealized active suspension with preview and without consideration the tire lift off effect is obtained:

$$\dot{\mathbf{x}}_\mathbf{a} = \mathbf{A_a}\mathbf{x_a} + \mathbf{B_a}u + \mathbf{G_{aw}}\dot{w} \tag{11}$$

where

$$\mathbf{A_a} = \begin{bmatrix} \mathbf{O_a} & \mathbf{T_{aA}} \\ \mathbf{-M_a^{-1}K_a} & \mathbf{O_a} \end{bmatrix} \tag{12}$$

The state vector $\boldsymbol{x_a}$ contains relative displacements $\mathbf{q_{aR}}$ (suspension and the tire deflections) and absolute velocities $\dot{\mathbf{q}}_{\mathbf{aA}}$ (car body and the wheel velocities) – see (8). Such a description leads to the velocity of road disturbances at the input. It is assumed that the road disturbances *w(t)* (and also its derivation) are measured at the distance l_p in front of the vehicle, i.e. at time t the preview information about incoming road disturbances is available from the time t up to time $t + t_p$, where $t_p = l_p/v$ is the preview time and v is the vehicle velocity. The active force generator is optimized in regard to ride comfort, suspension rattle space and road holding. Corresponding variables to be minimized are car body acceleration, suspension deflection and tire deflection.

$$\mathbf{z} = \begin{bmatrix} \ddot{y}_1 & y_1 - y_2 & y_2 - w \end{bmatrix}^T \tag{13}$$

and in state space form

$$\mathbf{z} = \mathbf{C_a}\mathbf{x_a} + \mathbf{D_a}u + \mathbf{H_a}\dot{w} \tag{14}$$

Then the performance index involves appropriately weighted variances of optimized variables (13) that are to be minimized and weighted variance of active force that is also to be minimized:

$$J = \lim_{T\to\infty}\frac{1}{T}\int_0^T \left[q_1\ddot{y}_1^2 + q_2\left(y_1 - y_2\right)^2 + q_3\left(y_2 - w\right)^2 + Ru^2 \right] dt \tag{15}$$

or using (13) in the generalized matrix form

$$J = \lim_{T\to\infty}\frac{1}{T}\int_0^T \left(\mathbf{z^T Q z} + u^\mathbf{T} R u\right) dt \tag{16}$$

where

$$\mathbf{Q} = \begin{bmatrix} q_1 & 0 & 0 \\ 0 & q_2 & 0 \\ 0 & 0 & q_3 \end{bmatrix} \tag{17}$$

Constants q_1, q_2 and q_3 are weighting constants chosen by the designer that determine the tradeoff between the optimized variables. **Q** is weighting matrix and R is control cost constant.

After substituting for **z**, the argument of the integral (16) after some adjustment has the form

$$\mathbf{z}^{\mathrm{T}}\mathbf{Q}\mathbf{z}+u^{\mathrm{T}}Ru=\mathbf{x}_{\mathbf{a}}^{\mathrm{T}}\mathbf{Q}_{\mathbf{1}}\mathbf{x}_{\mathbf{a}}+u^{\mathrm{T}}R_{1}u+\dot{w}^{\mathrm{T}}Q_{2}\dot{w}+2\mathbf{x}_{\mathbf{a}}^{\mathrm{T}}\mathbf{N}_{\mathbf{1}}u+2\mathbf{x}_{\mathbf{a}}^{\mathrm{T}}\mathbf{N}_{\mathbf{2}}\dot{w} \tag{18}$$

where

$$\mathbf{Q}_{\mathbf{1}}=\mathbf{C}_{\mathbf{a}}^{\mathrm{T}}\mathbf{Q}\mathbf{C}_{\mathbf{a}},\quad R_{1}=\mathbf{D}_{\mathbf{a}}^{\mathrm{T}}\mathbf{Q}\mathbf{D}_{\mathbf{a}}+R,\quad Q_{2}=\mathbf{H}_{\mathbf{a}}^{\mathrm{T}}\mathbf{Q}\mathbf{H}_{\mathbf{a}},\quad \mathbf{N}_{\mathbf{1}}=\mathbf{C}_{\mathbf{a}}^{\mathrm{T}}\mathbf{Q}\mathbf{D}_{\mathbf{a}}\quad \mathbf{N}_{\mathbf{2}}=\mathbf{C}_{\mathbf{a}}^{\mathrm{T}}\mathbf{Q}\mathbf{H}_{\mathbf{a}} \tag{19}$$

Then the Hamiltonian H for this issue is in the form

$$\mathbf{H}=\frac{1}{2}\left(\mathbf{x}_{\mathbf{a}}^{\mathrm{T}}\mathbf{Q}_{\mathbf{1}}\mathbf{x}_{\mathbf{a}}+u^{\mathrm{T}}R_{1}u+\dot{w}^{\mathrm{T}}Q_{2}\dot{w}+2\mathbf{x}_{\mathbf{a}}^{\mathrm{T}}\mathbf{N}_{\mathbf{1}}u+2\mathbf{x}_{\mathbf{a}}^{\mathrm{T}}\mathbf{N}_{\mathbf{2}}\dot{w}\right)+\boldsymbol{\lambda}^{\mathrm{T}}\left(\mathbf{A}_{\mathbf{a}}\mathbf{x}_{\mathbf{a}}+\mathbf{B}_{\mathbf{a}}u+\mathbf{G}_{\mathbf{aw}}\dot{w}-\dot{\mathbf{x}}_{\mathbf{a}}\right) \tag{20}$$

where $\boldsymbol{\lambda}$ is a vector of Lagrange multipliers. The necessary conditions for the optimum of **H** are

$$\frac{\partial\mathbf{H}}{\partial u}=0\quad\wedge\quad\frac{d}{dt}\left(\frac{\partial\mathbf{H}}{\partial\dot{\mathbf{x}}_{\mathbf{a}}}\right)=-\frac{\partial\mathbf{H}}{\partial\mathbf{x}_{\mathbf{a}}} \tag{21}$$

From the first condition we obtain the active control force u

$$\frac{\partial\mathbf{H}}{\partial u}=0:\quad u^{\mathrm{T}}R_{1}+\mathbf{x}_{\mathbf{a}}^{\mathrm{T}}\mathbf{N}_{\mathbf{1}}+\boldsymbol{\lambda}^{\mathrm{T}}\mathbf{B}_{\mathbf{a}}=0\quad\Rightarrow\quad u=-R_{1}^{-1}\left(\mathbf{N}_{\mathbf{1}}^{\mathrm{T}}\mathbf{x}_{\mathbf{a}}+\mathbf{B}_{\mathbf{a}}^{\mathrm{T}}\boldsymbol{\lambda}\right) \tag{22}$$

From the second necessary condition

$$\frac{d}{dt}\left(\frac{\partial\mathbf{H}}{\partial\dot{\mathbf{x}}_{\mathbf{a}}}\right)=-\frac{\partial\mathbf{H}}{\partial\mathbf{x}_{\mathbf{a}}}:\quad\dot{\boldsymbol{\lambda}}^{\mathrm{T}}=-\left(\mathbf{x}_{\mathbf{a}}^{\mathrm{T}}\mathbf{Q}_{\mathbf{1}}+u^{\mathrm{T}}\mathbf{N}_{\mathbf{1}}^{\mathrm{T}}+\dot{w}^{\mathrm{T}}\mathbf{N}_{\mathbf{2}}^{\mathrm{T}}+\boldsymbol{\lambda}^{\mathrm{T}}\mathbf{A}_{\mathbf{a}}\right) \tag{23}$$

After substituting the control force – in relation (22) – into (23) and after some adjustment we obtain

$$\dot{\boldsymbol{\lambda}}=-\left(\mathbf{Q}_{\mathbf{n}}\mathbf{x}_{\mathbf{a}}+\mathbf{A}_{\mathbf{n}}^{\mathrm{T}}\boldsymbol{\lambda}+\mathbf{N}_{\mathbf{2}}\dot{w}\right) \tag{24}$$

where

$$\mathbf{Q}_{\mathbf{n}}=\mathbf{Q}_{\mathbf{1}}-\mathbf{N}_{\mathbf{1}}R_{1}^{-1}\mathbf{N}_{\mathbf{1}}^{\mathrm{T}},\quad\mathbf{A}_{\mathbf{n}}=\mathbf{A}_{\mathbf{a}}-\mathbf{B}_{\mathbf{a}}R_{1}^{-1}\mathbf{N}_{\mathbf{1}}^{\mathrm{T}} \tag{25}$$

Substitution the control force – in relation (22) – into the state equation (11) gives

$$\dot{\mathbf{x}}_{\mathbf{a}}=\mathbf{A}_{\mathbf{n}}\mathbf{x}_{\mathbf{a}}-\mathbf{B}_{\mathbf{a}}R_{1}^{-1}\mathbf{B}_{\mathbf{a}}^{\mathrm{T}}\boldsymbol{\lambda}+\mathbf{G}_{\mathbf{aw}}\dot{w} \tag{26}$$

From the linear structure of equations (24) and (26) the proposed solution follows

$$\boldsymbol{\lambda}(t)=\mathbf{P}(t)\mathbf{x}_{\mathbf{a}}(t)+\mathbf{r}(t) \tag{27}$$

where

$$\mathbf{P}(T)=\mathbf{P}_{\mathbf{T}},\quad\mathbf{r}(T)=0,\quad\boldsymbol{\lambda}(T)=\mathbf{P}_{\mathbf{T}}\mathbf{x}_{\mathbf{a}}(T) \tag{28}$$

where $\mathbf{r}(t)$ is a vector dependent on the excitation $\dot{w}(t)$ and T is the duration of the problem. Differentiation (27) according to time gives

$$\dot{\boldsymbol{\lambda}}(t)=\dot{\mathbf{P}}(t)\mathbf{x}_{\mathbf{a}}(t)+\mathbf{P}(t)\dot{\mathbf{x}}_{\mathbf{a}}(t)+\dot{\mathbf{r}}(t) \tag{29}$$

Substitution the relations (27) into (26) and next (24) and (26) into (29) after some manipulation yields

$$\left(\dot{\mathbf{P}}+\mathbf{P}\mathbf{A}_{\mathbf{n}}+\mathbf{A}_{\mathbf{n}}^{\mathrm{T}}\mathbf{P}-\mathbf{P}\mathbf{B}_{\mathbf{a}}R_{1}^{-1}\mathbf{B}_{\mathbf{a}}^{\mathrm{T}}\mathbf{P}+\mathbf{Q}_{\mathbf{n}}\right)\mathbf{x}_{\mathbf{a}}=-\dot{\mathbf{r}}+\left(-\mathbf{A}_{\mathbf{n}}^{\mathrm{T}}+\mathbf{P}\mathbf{B}_{\mathbf{a}}R_{1}^{-1}\mathbf{B}_{\mathbf{a}}^{\mathrm{T}}\right)\mathbf{r}-\left(\mathbf{P}\mathbf{G}_{\mathbf{aw}}+\mathbf{N}_{\mathbf{2}}\right)\dot{w} \tag{30}$$

Whereas $\mathbf{x}_{\mathbf{a}}(t)$ and $\dot{w}(t)$ are arbitrary vectors, relation (30) is valid only when both sides of (30) are zero vectors, which implies

$$\begin{aligned}-\dot{\mathbf{P}}&=\mathbf{P}\mathbf{A}_{\mathbf{n}}+\mathbf{A}_{\mathbf{n}}^{\mathrm{T}}\mathbf{P}-\mathbf{P}\mathbf{B}_{\mathbf{a}}R_{1}^{-1}\mathbf{B}_{\mathbf{a}}^{\mathrm{T}}\mathbf{P}+\mathbf{Q}_{\mathbf{n}}\\ \dot{\mathbf{r}}&=\left(-\mathbf{A}_{\mathbf{n}}^{\mathrm{T}}+\mathbf{P}\mathbf{B}_{\mathbf{a}}R_{1}^{-1}\mathbf{B}_{\mathbf{a}}^{\mathrm{T}}\right)\mathbf{r}-\left(\mathbf{P}\mathbf{G}_{\mathbf{aw}}+\mathbf{N}_{\mathbf{2}}\right)\dot{w},\quad\mathbf{r}(T)=0\end{aligned} \tag{31}$$

If the problem duration T approaches infinity, $T \to \infty$, the first equation from relations (31) can be rewritten as

$$\mathbf{P}\mathbf{A}_\mathbf{n} + \mathbf{A}_\mathbf{n}^\mathbf{T}\mathbf{P} - \mathbf{P}\mathbf{B}_\mathbf{a} R_1^{-1} \mathbf{B}_\mathbf{a}^\mathbf{T}\mathbf{P} + \mathbf{Q}_\mathbf{n} = \mathbf{O} \tag{32}$$

where now $\mathbf{P}$ is a nonnegative definite symmetric solution of the algebraic Riccati equation (32).
The second equation from relations (31) is integrated backwards and uses all the future information about the derivative of the road input $\dot{w}(t)$ up to time $t = T$. Nevertheless $\dot{w}(t)$ for $\tau > t + t_p$ is not available, because at time t the preview information about incoming road disturbances is available from the time t only up to time $t + t_p$, therefore $\dot{w}(t)$ for $\tau > t + t_p$ is replaced by its expectation which is zero. This yields zero solution for $\mathbf{r}(\tau)$ for $\tau \geq t + t_p$.

$$\dot{\mathbf{r}} = \left(-\mathbf{A}_\mathbf{n}^\mathbf{T} + \mathbf{P}\mathbf{B}_\mathbf{a} R_1^{-1} \mathbf{B}_\mathbf{a}^\mathbf{T}\right)\mathbf{r} - \left(\mathbf{P}\mathbf{G}_\mathbf{aw} + \mathbf{N}_\mathbf{2}\right)\dot{w}, \quad \mathbf{r}\left(t + t_p\right) = 0 \tag{33}$$

After some substitutions

$$\dot{\mathbf{r}} = -\mathbf{A}_\mathbf{c}^\mathbf{T}\mathbf{r} - \mathbf{G}_\mathbf{r}\dot{w}, \quad \mathbf{r}\left(t + t_p\right) = 0 \tag{34}$$

where

$$\mathbf{A}_\mathbf{c} = \mathbf{A}_\mathbf{n} - \mathbf{B}_\mathbf{a} R_1^{-1} \mathbf{B}_\mathbf{a}^\mathbf{T}\mathbf{P}, \quad \mathbf{G}_\mathbf{r} = \mathbf{P}\mathbf{G}_\mathbf{aw} + \mathbf{N}_\mathbf{2} \tag{35}$$

The solution of equation (34) is given by following integral:

$$\mathbf{r}(t) = e^{-\mathbf{A}_\mathbf{c}^\mathbf{T} t}\left[\mathbf{c}_\mathbf{r} - \int_1^t e^{\mathbf{A}_\mathbf{c}^\mathbf{T}\tau}\mathbf{G}_\mathbf{r}\dot{w}(\tau)d\tau\right] \tag{36}$$

With respect to $\mathbf{r}(t + t_p) = 0$, the vector integration constant $\mathbf{c}_r$ is obtained

$$\mathbf{o} = e^{-\mathbf{A}_\mathbf{c}^\mathbf{T}\left(t+t_p\right)}\left[\mathbf{c}_\mathbf{r} - \int_1^{t+t_p} e^{\mathbf{A}_\mathbf{c}^\mathbf{T}\tau}\mathbf{G}_\mathbf{r}\dot{w}(\tau)d\tau\right] \;\Rightarrow\; \mathbf{c}_\mathbf{r} = \int_1^{t+t_p} e^{\mathbf{A}_\mathbf{c}^\mathbf{T}\tau}\mathbf{G}_\mathbf{r}\dot{w}(\tau)d\tau \tag{37}$$

Substituting $\mathbf{c}_r$ obtained in (37) into (36) after some manipulations gives

$$\mathbf{r}(t) = \int_t^{t+t_p} e^{\mathbf{A}_\mathbf{c}^\mathbf{T}(\tau - t)}\mathbf{G}_\mathbf{r}\dot{w}(\tau)d\tau \tag{38}$$

Now, state a substitution $\sigma = \tau - t$. Integral (38) after performing the substitution and switching the limits of integration is transferred to form

$$\mathbf{r}(t) = \int_0^{t_p} e^{\mathbf{A}_\mathbf{c}^\mathbf{T}\sigma}\mathbf{G}_\mathbf{r}\dot{w}(t + \sigma)d\sigma \tag{39}$$

For determination of $\mathbf{r}(t)$ it is necessary to solve the integral (39) at each time.
Finally, substituting $\boldsymbol{\lambda}$ – equation (27) – into the one for the control force – equation (22) – and with respect to (32) and (39), after some manipulations, the active control force is obtained

$$u = -R_1^{-1}\left(\mathbf{N}_\mathbf{1}^\mathbf{T} + \mathbf{B}_\mathbf{a}^\mathbf{T}\mathbf{P}\right)\mathbf{x}_\mathbf{a} - R_1^{-1}\mathbf{B}_\mathbf{a}^\mathbf{T}\mathbf{r} \tag{40}$$

After the introduction of substitutions

$$\mathbf{K}_\mathbf{b} = R_1^{-1}\left(\mathbf{N}_\mathbf{1}^\mathbf{T} + \mathbf{B}_\mathbf{a}^\mathbf{T}\mathbf{P}\right), \quad \mathbf{K}_\mathbf{f} = R_1^{-1}\mathbf{B}_\mathbf{a}^\mathbf{T} \tag{41}$$

the relation (40) has the form

$$u = -\mathbf{K}_\mathbf{b}\mathbf{x}_\mathbf{a} - \mathbf{K}_\mathbf{f}\mathbf{r} \tag{42}$$

It can be seen that the active control force consists of the feedback gain $\mathbf{K}_\mathbf{b}$ and of the feedforward gain $\mathbf{K}_\mathbf{f}$. The feedforward part of the active control force $\mathbf{K}_\mathbf{f}\mathbf{r}(t)$ is a function of incoming road disturbances – integral (39) – which implies that it tries to eliminate the effect of these approaching road excitation on the vehicle.

With respect to (42), the state equation (11) of idealized fully active system can be rewritten as

$$\dot{\mathbf{x}}_\mathbf{a} = \left(\mathbf{A}_\mathbf{a} - \mathbf{B}_\mathbf{a}\mathbf{K}_\mathbf{b}\right)\mathbf{x}_\mathbf{a} - \mathbf{B}_\mathbf{a}\mathbf{K}_\mathbf{f}\mathbf{r} + \mathbf{G}_\mathbf{aw}\dot{w} \tag{43}$$

4. MR damper – hydromechanical and mathematical model

Hydromechanical and mathematical model of the MR damper were identified by the author in publication (Úradníček, 2008), where they were designed on the basis of model of an electrorheological damper compiled in publication (Hong & Choi, 2005).

Hydromechanical parameters of the hydromechanical model of the MR damper – figure 2 a) – are:
C_1, C_2, C_4 – compressibility of the volumes front of, behind the piston and of gas storage
A_1, A_2, A_4, A_f – cross-sectional area of the bottom, top part of the piston and cross-sectional area of the membrane and of the grooves
p_1, p_2, p_4 – pressures of the MR fluid front of, behind the piston and of gas storage
I_f – inertia of the MR fluid flowing through the grooves of the piston
R_f – hydraulic resistance of the MR fluid flowing through the groove of the piston
Δp_{MR} – pressure drop in the groove of the piston caused by friction force
y_r – displacement of the MR fluid flowing through the groove of the piston relative to piston
y_p – displacement of the piston of the MR damper
y_m – displacement of the membrane separating the MR fluid from gas
Overall pressure drop in front of and behind the piston is:

$$\Delta p = p_2 - p_1 = I_f A_f \ddot{y}_r + R_f A_f \dot{y}_r + \Delta p_{MR} \tanh\left(\beta_d \dot{y}_r\right) \tag{44}$$

The parameter β_d allows us to regulate the friction force near zero velocity of motion of the MR fluid flowing through the grooves. The function tanh (-) ensures the consistency of the mathematical model.

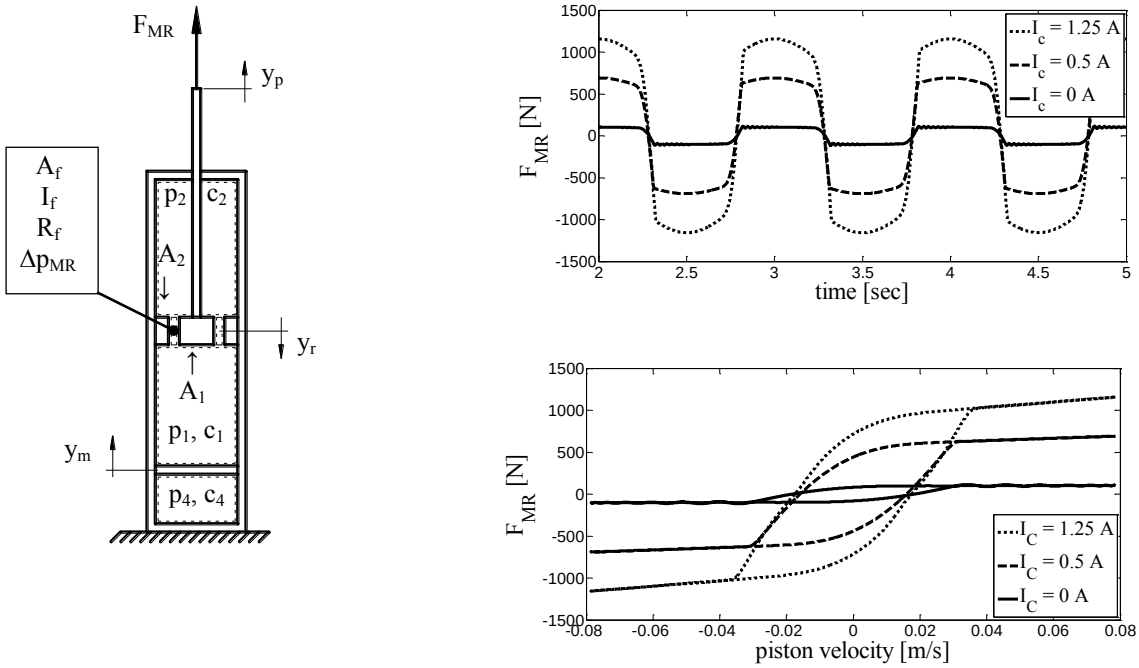

a.) *b.)*

Fig. 2: a.) hydromechanical model of the MR damper b.) dynamical characteristics of the MR damper

Maintain the continuity of the volumes front of, behind the piston and of gas storage describe following relations:

$$\begin{aligned} c_1 p_1 &= -\left(A_1 - A_f\right) y_p + A_f y_r + A_4 y_m \\ c_2 p_2 &= \left(A_2 - A_f\right) y_p - A_f y_r \\ c_4 p_4 &= A_4 y_m \end{aligned} \tag{45}$$

Since the cross-sectional areas A_1 and A_2 are approximately equal, they can be approximated by their mean value $A_p \approx (A_1 + A_2) / 2$.
Pressures in front of the piston and of gas storage are also approximately equal – $p_1 \approx p_4$.

Pressure drop in front of and behind the piston with respect to relations (45) and the above assumptions after some manipulation is:

$$p_2 - p_1 = -A_f \left(\frac{1}{c_1 + c_4} + \frac{1}{c_2} \right) y_r + \left(A_p - A_f \right) \left(\frac{1}{c_1 + c_4} + \frac{1}{c_2} \right) y_p \tag{46}$$

By substituting the equation (46) into (44) and by multiplying by the approximate area, the equation of motion of the hydromechanical model of the MR damper in the figure 2 a.) is obtained.

$$I_f A_f A_p \ddot{y}_r + R_f A_f A_p \dot{y}_r + \Delta p_{MR} A_p \tanh\left(\beta_d \dot{y}_r\right) + A_f \left(\frac{1}{c_1 + c_4} + \frac{1}{c_2} \right) A_p y_r = \left(A_p - A_f \right) \left(\frac{1}{c_1 + c_4} + \frac{1}{c_2} \right) y_p \tag{47}$$

After substitutions

$$\begin{aligned} &m_f = I_f A_f A_p, \quad c_f = R_f A_f A_p, \quad F_y = \Delta p_{MR} A_p, \\ &k_{f_1} = A_f \left(\frac{1}{c_1 + c_4} + \frac{1}{c_2} \right) A_p, \quad k_{f_2} = \left(A_p - A_f \right) \left(\frac{1}{c_1 + c_4} + \frac{1}{c_2} \right) \end{aligned} \tag{48}$$

the equation of motion (47) is transferred to form

$$m_f \ddot{y}_r + c_f \dot{y}_r + F_y \tanh\left(\beta_d \dot{y}_r\right) + k_{f_1} y_r = k_{f_2} y_p \tag{49}$$

The damping force of the MR damper is proportional to the pressure difference in front of and behind the piston

$$F_{MR} = \left(p_2 - p_1 \right) A_p \tag{50}$$

By substituting (44) into (50) with respect to substitutions (48) the damping force of the MR damper is obtained

$$F_{MR} = m_f \ddot{y}_r + c_f \dot{y}_r + F_y \tanh\left(\beta_d \dot{y}_r\right) \tag{51}$$

With respect to the equation of motion (49) for the damping force also applies

$$F_{MR} = k_{f_2} y_p - k_{f_1} y_r \tag{52}$$

In publication (Úradníček, 2008) author experimentally identified the parameters of the MR damper LORD RD – 1005 – 3 on the basis of mathematical model described by relations (49) and (51) as functions of electric current flowing through the coil of the MR damper (for the range of electric current 0 – 1.25 A):

$$\begin{aligned} &m_f = d_5 \qquad c_f\left(I_c\right) = c_1 I_c + d_1 \qquad F_y\left(I_c\right) = a_2 I_c^3 + b_2 I_c^2 + c_2 I_c + d_2 \\ &\beta_d = 80 \qquad k_{f_1}\left(I_c\right) = b_3 I_c^2 + c_3 I_c + d_3 \qquad k_{f_2}\left(I_c\right) = b_4 I_c^2 + c_4 I_c + d_4 \end{aligned} \tag{53}$$

The values of the parameters of the approximate functions (53) are in the table 1.

Tab. 1: Values of the parameters of the approximate functions (53)

i	a_i	b_i	c_i	d_i
1	0	0	1685	21.5
2	- 368.19	216.5	952.02	98.61
3	0	- 772967.93	1657383.84	76527.7
4	0	- 1271919	2571391.71	173556.34
5	0	0	0	1.45

Some dynamical characteristics of the identified mathematical model of the MR damper – equations (49) and (51) – excited by a harmonic force of amplitude *12.5 mm* and frequency *1 Hz* for different electric currents are in the figure 2 b.).

5. Quarter car model with MR damper and with consideration the tire lift off

The mathematical model of the semi-active MR damper described in the previous section is implemented in the quarter car model described in the second section. So the idealized fully active suspension is replaced by the MR damper. In the equations of motion (1) the active control force u is replaced by the one generated by the MR damper – F_{MR}.

$$\begin{aligned} m_1\ddot{y}_1 &= -k_1\left(y_1 - y_2\right) + F_{MR} - m_1 g \\ m_2\ddot{y}_2 &= -k_2\left(y_2 - w\right)\left[1 - H\left(y_2 - w\right)\right] - k_1\left(y_2 - y_1\right) - F_{MR} - m_2 g \end{aligned} \tag{54}$$

Dynamics of the MR damper is described by the relations (49) and (51) in the previous section. It is useful to utilize the relation (52) instead of the relation (51) for the expression of the damping force of the MR damper.

$$\begin{aligned} m_f\ddot{y}_r + c_f\dot{y}_r + F_y \tanh\left(\beta_d\dot{y}_r\right) + k_{f_1} y_r &= k_{f_2} y_p \\ F_{MR} &= k_{f_2} y_p - k_{f_1} y_r \end{aligned} \tag{55}$$

In the case of using the MR damper in the quarter car suspension the piston displacement y_p with respect to the figure 2 a.) and equations of motion (54) is replaced by the suspension deflection $y_2 - y_1$.

$$\begin{aligned} m_f\ddot{y}_r + c_f\dot{y}_r + F_y \tanh\left(\beta_d\dot{y}_r\right) + k_{f_1} y_r &= -k_{f_2}\left(y_1 - y_2\right) \\ F_{MR} &= -k_{f_2}\left(y_1 - y_2\right) - k_{f_1} y_r \end{aligned} \tag{56}$$

By substituting the MR damping force from the second relation of (56) into (54) the equations of motion of the quarter car model with MR damper and with consideration the tire lift off in the matrix form are

$$\mathbf{M_s}\ddot{\mathbf{q}}_{\mathbf{sA}} + \mathbf{B_{sL}}\dot{\mathbf{q}}_{\mathbf{sA}} + \mathbf{B}_{s\mathbf{N}} \tanh\left(\beta_d\dot{\mathbf{q}}_{\mathbf{sA}}\right) + \mathbf{K_{sL}}\mathbf{q_{sR}} + \mathbf{K_{sN}}\mathbf{q_{sR}}\mathbf{e_s} \tanh\left(\beta_r\mathbf{q_{sR}}\right) = \mathbf{b_{sg}} g \tag{57}$$

where

$$\mathbf{M_s} = \begin{bmatrix} m_1 & 0 & 0 \\ 0 & m_2 & 0 \\ 0 & 0 & m_f \end{bmatrix},\ \mathbf{B_{sL}} = \begin{bmatrix} 0 & 0 & 0 \\ 0 & 0 & 0 \\ 0 & 0 & c_f \end{bmatrix},\ \mathbf{B_{sN}} = \begin{bmatrix} 0 & 0 & 0 \\ 0 & 0 & 0 \\ 0 & 0 & F_y \end{bmatrix},\ \mathbf{K_{sN}} = \begin{bmatrix} 0 & 0 & 0 \\ 0 & -k_2/2 & 0 \\ 0 & 0 & 0 \end{bmatrix} \tag{58}$$

$$\mathbf{K_{sL}} = \begin{bmatrix} k_1 + k_{f_2} & 0 & k_{f_1} \\ -\left(k_1 + k_{f_2}\right) & \dfrac{k_2}{2} & -k_{f_1} \\ k_{f_2} & 0 & k_{f_1} \end{bmatrix},\ \mathbf{e_s} = \begin{bmatrix} 0 \\ 1 \\ 0 \end{bmatrix}^T,\ \mathbf{b_{sg}} = -\begin{bmatrix} m_1 \\ m_2 \\ 0 \end{bmatrix},\ \mathbf{q_{sA}} = \begin{bmatrix} y_1 \\ y_2 \\ y_r \end{bmatrix},\ \mathbf{q_{sR}} = \begin{bmatrix} y_1 - y_2 \\ y_2 - w \\ y_r \end{bmatrix}$$

Transformation from absolute to the relative coordinates is realized through the equation:

$$\mathbf{q_{sR}} = \mathbf{T_{sA}}\mathbf{q_{sA}} + \mathbf{T_{sw}} w \tag{59}$$

where

$$\mathbf{T_{sA}} = \begin{bmatrix} 1 & -1 & 0 \\ 0 & 1 & 0 \\ 0 & 0 & 1 \end{bmatrix},\ \mathbf{T_{sw}} = \begin{bmatrix} 0 \\ -1 \\ 0 \end{bmatrix} \tag{60}$$

Combining equation (57) and differentiated equation (59), state space model is obtained:

$$\dot{\mathbf{x}}_\mathbf{s} = \mathbf{A_{sL}}\mathbf{x_s} + \mathbf{A_{sr}}\mathbf{x_s}\mathbf{E_s} \tanh\left(\beta_r\mathbf{x_s}\right) + \mathbf{A_{sd}} \tanh\left(\beta_d\mathbf{x_s}\right) + \mathbf{G_s}\mathbf{f_{gw}} \tag{61}$$

where

$$\mathbf{A}_{\mathbf{sL}}=\begin{bmatrix}\mathbf{O}_{\mathbf{s}} & \mathbf{T}_{\mathbf{sA}}\\ -\mathbf{M}_{\mathbf{s}}^{-1}\mathbf{K}_{\mathbf{sL}} & -\mathbf{M}_{\mathbf{s}}^{-1}\mathbf{B}_{\mathbf{sL}}\end{bmatrix},\quad \mathbf{A}_{\mathbf{sr}}=\begin{bmatrix}\mathbf{O}_{\mathbf{s}} & \mathbf{O}_{\mathbf{s}}\\ -\mathbf{M}_{\mathbf{s}}^{-1}\mathbf{K}_{\mathbf{sN}} & \mathbf{O}_{\mathbf{s}}\end{bmatrix},\quad \mathbf{A}_{\mathbf{sd}}=\begin{bmatrix}\mathbf{O}_{\mathbf{s}} & \mathbf{O}_{\mathbf{s}}\\ \mathbf{O}_{\mathbf{s}} & -\mathbf{M}_{\mathbf{s}}^{-1}\mathbf{B}_{\mathbf{sN}}\end{bmatrix}$$
$$\mathbf{E}_{\mathbf{s}}=\begin{bmatrix}\mathbf{e}_{\mathbf{s}}^{T}\\ \mathbf{o}_{\mathbf{s}}\end{bmatrix}^{T},\quad \mathbf{G}_{\mathbf{s}}=\begin{bmatrix}\mathbf{G}_{\mathbf{sg}} & \mathbf{G}_{\mathbf{sw}}\end{bmatrix},\quad \mathbf{G}_{\mathbf{sg}}=\begin{bmatrix}\mathbf{o}_{\mathbf{s}}\\ \mathbf{M}_{\mathbf{s}}^{-1}\mathbf{b}_{\mathbf{sg}}\end{bmatrix},\quad \mathbf{G}_{\mathbf{sw}}=\begin{bmatrix}\mathbf{T}_{\mathbf{sw}}\\ \mathbf{o}_{\mathbf{s}}\end{bmatrix},\quad \mathbf{x}_{\mathbf{s}}=\begin{bmatrix}\mathbf{q}_{\mathbf{sR}}\\ \dot{\mathbf{q}}_{\mathbf{sA}}\end{bmatrix} \tag{62}$$

where $\mathbf{O}_{\mathbf{s}}$ and $\mathbf{o}_{\mathbf{s}}$ are zero matrix and vector respectively of appropriate dimensions.

6. Continuous inverse mathematical model of the MR damper

Mathematical model of the MR damper works such – see relations (56) – that for given electric current and for kinematic variables the damping force F_{MR} is calculated. An inverse model of the MR damper designed for the use of control should calculate the control electric current for given kinematic variables and for required damping force.

In section 3 the optimal preview control and corresponding active control force were derived. In this section as required damping force F_{MR} that is trying to be matched by the MR damper the active control force u from section 3 is taken. In some situations the active force is physically unable to be achieved by the MR damper. This problem is solved below.
As it was pointed out the active control force that would be generated by fully active system is trying to be matched by the one generated by the MR damper, so with respect to the second relation of (56) it can be written

$$\begin{aligned} F_{MR} &= u\\ -k_{f_2}\left(y_1-y_2\right)-k_{f_1}y_r &= u\end{aligned} \tag{63}$$

For the use of control it is appropriate to replace the variables $k_{f1}(I_c)$ and $k_{f2}(I_c)$ from relations (53) by linear functions $k_{f1r}(I_r)$ and $k_{f2r}(I_r)$ and for given range of control electric current to optimize their parameters by the least squares method – see figure (3)

$$k_{f_{1r}}\left(I_r\right)=c_{3r}I_r+d_{3r},\qquad k_{f_{2r}}\left(I_r\right)=c_{4r}I_r+d_{4r} \tag{64}$$

These relations (64) are used only in the inverse model of the MR damper for calculating the required electric current.

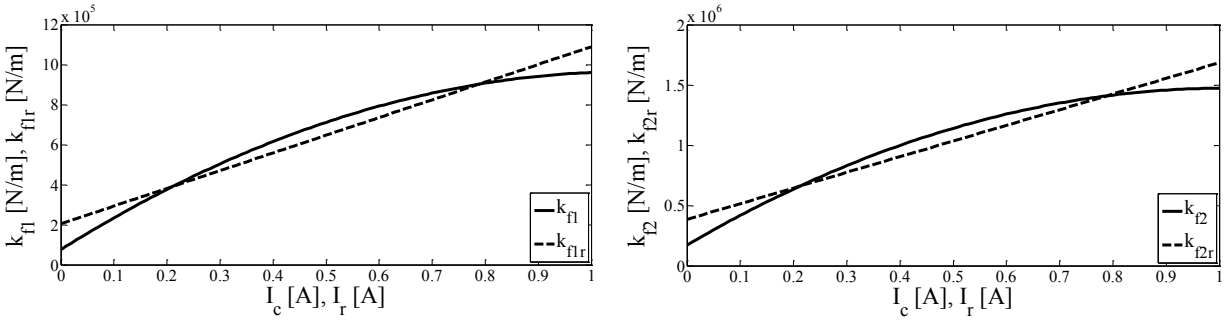

Fig. 3: Comparison of the functions used in the mechanical and in the inverse model of the MR damper see relations (53) and (64

After mentioned replacement the second relation of (63) now has the form

$$-k_{f_{2r}}\left(y_1-y_2\right)-k_{f_{1r}}y_r=u \tag{65}$$

By substituting (64) and (42) – relation for calculating the active control force u – into (65) we obtain

$$\begin{aligned} &-\left(c_{4r}I_r+d_{4r}\right)\left(y_1-y_2\right)-\left(c_{3r}I_r+d_{3r}\right)y_r=\\ &=-K_{b_1}\left(y_1-y_2\right)-K_{b_2}\left(y_2-w\right)-K_{b_3}\dot{y}_1-K_{b_4}\dot{y}_2-\mathbf{K}_{\mathbf{f}}\mathbf{r}\end{aligned} \tag{66}$$

where

$$\mathbf{K_b} = \begin{bmatrix} K_{b_1} & K_{b_2} & K_{b_3} & K_{b_4} \end{bmatrix}^T, \quad \mathbf{x_a} = \begin{bmatrix} y_1 - y_2 & y_2 - w & \dot{y}_1 & \dot{y}_2 \end{bmatrix}^T \tag{67}$$

After some manipulations the required control electric current is obtained

$$I_r = \frac{\left(\mathbf{K_{I_n}} + \mathbf{K_{b_s}}\right)\mathbf{x_s} + \mathbf{K_f r}}{\mathbf{K_{I_d}} \mathbf{x_s}} \tag{68}$$

where

$$\begin{aligned} \mathbf{K_{I_n}} &= \begin{bmatrix} -d_{4r} & 0 & -d_{3r} & 0 & 0 & 0 \end{bmatrix}, \quad \mathbf{K_{b_s}} = \begin{bmatrix} K_{b_1} & K_{b_2} & 0 & K_{b_3} & K_{b_4} & 0 \end{bmatrix} \\ \mathbf{K_{I_d}} &= \begin{bmatrix} c_{4r} & 0 & c_{3r} & 0 & 0 & 0 \end{bmatrix}, \quad \mathbf{x_s} = \begin{bmatrix} y_1 - y_2 & y_2 - w & y_r & \dot{y}_1 & \dot{y}_2 & \dot{y}_r \end{bmatrix}^T \end{aligned} \tag{69}$$

If this fictive required electric current I_r flew through the coil of the MR damper, the ideal control active force would be achieved. The required electric current I_r calculated from the relation (68) can be any real number (also negative, which is physically impossible). But there are some restrictions of electric control current. Working range of the electric current is limited to *0 – 1 A*. Instead of commonly used saturation a continuous function is utilized for the calculation of theoretical control electric current for used MR damper (Havelka, 2010) – see figure 4

$$I_{ct} = \frac{1}{2}\left\{1 + \tanh\left[\alpha\left(I_r - \frac{1}{2}\right)\right]\right\} \tag{70}$$

The parameter α was optimized by the least squares method to match the commonly used saturation.

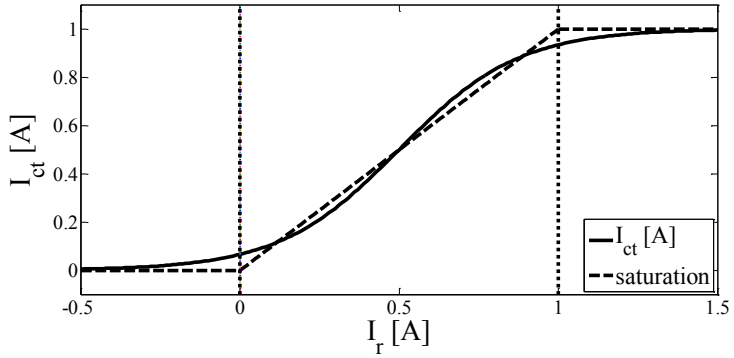

Fig. 4: Comparison of commonly used saturation and the designed continuous function I_{ct} [A]

Since the response time of an actual MR damper to the theoretical required control electric current I_{ct} is not immediate but time-delayed, this effect can be included into the model using a first order filter

$$\dot{I}_c(t) = -\frac{1}{T_{MR}}\left[I_c(t) - I_{ct}(t)\right] \tag{71}$$

where T_{MR} is the time constant of the MR damper set to *20 ms* and I_c is the actual electric current applied to the model (53) of the MR damper. It further means that the system matrices $\mathbf{A_{sL}}$ and $\mathbf{A_{sd}}$ of the state space model (61) are also dependent on the applied electric current I_c.

7. Simulations and results

To significantly demonstrate the benefits of preview control the vehicle model was let to travel over a bump and further it was supposed that all the state variables are measured. The bump is described by equation

$$w(t) = \left\{H\left(t - t_{bs}\right) - H\left[t - \left(t_{bs} + t_b\right)\right]\right\}\frac{b_h}{2}\left\{1 - \cos\left[2\pi\frac{1}{t_b}\left(t - t_{bs}\right)\right]\right\} \tag{72}$$

where t_{bs} is the "starting" time of the bump, b_h is the height of the bump and $t_b = b_l / v$ is the duration time of the bump where v is the vehicle velocity.

Values used during the simulations are listed below.

Bump parameters: $b_l = 0.5\ m;\ b_h = 0.05\ m$

Quarter car parameters: $m_1 = 288.9\ kg;\ m_2 = 28.58\ kg;\ k_1 = 14\ 000\ N/m;\ k_2 = 155\ 900\ N/m;$

Weighting constants: weight to ride comfort $q_1 = 1;$ weight to suspension rattle space $q_2 = 10^3;$
weight to road holding $q_3 = 10^4;$
weight to penalizing the active control force $r = 0$

Control electric current calculation: $c_{3r} = 884\ 415;\ d_{3r} = 205\ 355;\ c_{4r} = 1\ 299\ 475;\ d_{4r} = 385\ 540;$
$\alpha = 2.65$

The quarter car equipped with fully active idealized suspension was let to travel over a bump at velocity *4 m/s* – figure 5. The preview distance in front of the front wheel was set to *1.6 m*. This implies the preview time $t_p = 0.4\ sec.$

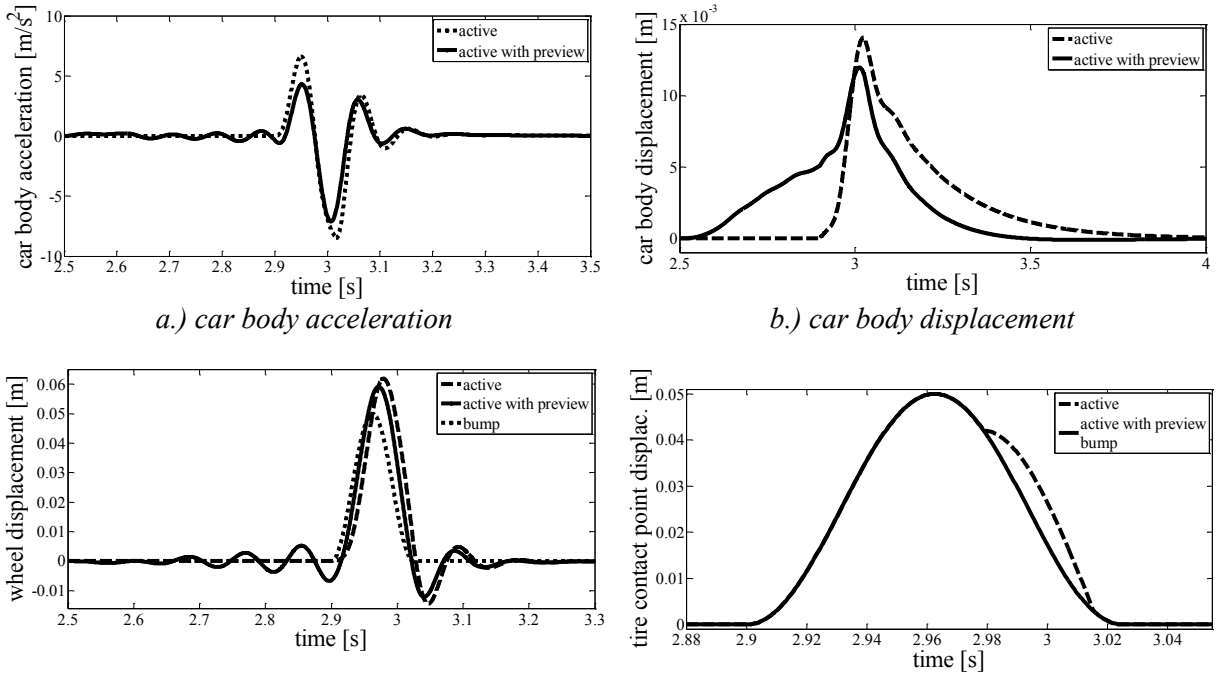

a.) car body acceleration *b.) car body displacement*

c.) wheel displacement *d.) tire contact point diplacement*

Fig. 5: Responses of the quarter car model traveling over a bump equipped with fully active system controlled by "active" and "active with preview" control strategies

In Figure 5 car body acceleration and car body, wheel and tire contact point displacements of fully active quarter car model traveling over a bump controlled by "active" and "active with preview" control strategies are shown. In all cases the active preview control strategy provides lower amplitudes and also smaller variances. As shown in Figure 5 c.) – the preview controlled active suspension acts the wheel before the bump excitation comes to smoothly lift it over the bump and avoids the tire lift off the road compared with the no preview case when the undesired tire lift off effect occurs – Figure 5 d.).

Then the quarter car equipped with the MR damper in suspension was let to travel over a bump at velocity *3.5 m/s* – figure 6. The preview distance in front of the front wheel was set to *1.6 m*. This implies the preview time $t_p = 0.457\ sec.$

Figure 6 shows that the semi-active MR damper with the preview case provides some small improvement in car body displacement compared with the no preview case, but in terms of the wheel displacement no difference between the preview and no preview case can be observed.

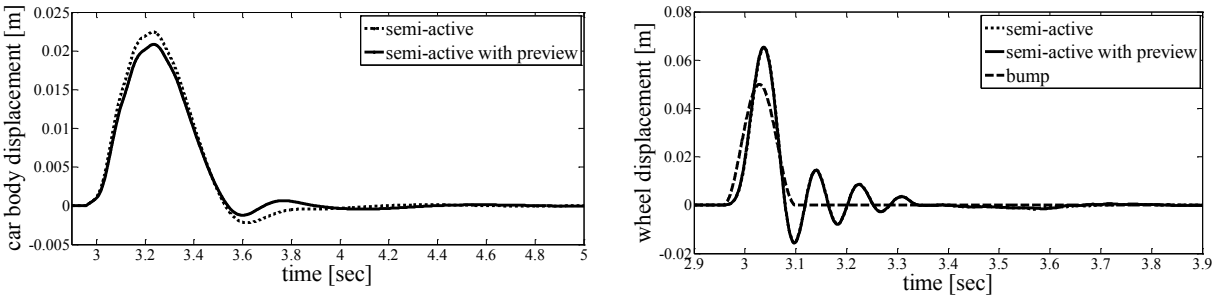

a.) car body displacement *b.) wheel displacement*

Fig.6: Responses of the quarter car model traveling over a bump equipped with MR damper controlled with "no preview" and "preview" control strategies

This is because the semi-active MR damper is unable to supply energy into the system and cannot generate forces when there is no changing suspension deflection, i.e. the MR damper cannot act the system before the excitation comes – see figure 7 b.).

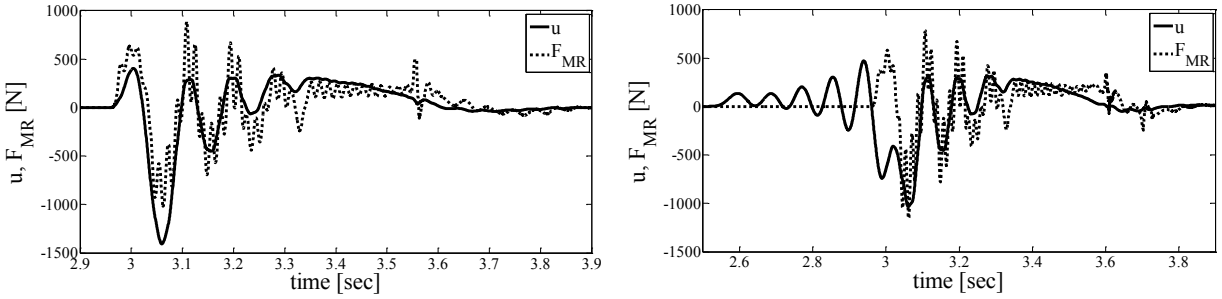

a.) no preview case *b.) preview case*

Fig.7: Required active force "u" and the actual control force of the MR damper "F_{MR}" in the quarter car model traveling over a bump controlled with" no preview" and "preview" control strategies

The control electric current is trying to change the MR fluid properties to achieve the required active control force – see figures 8 and 7 b.) from the time *2.5 sec* up to time *3 sec* – but during this time period there is no changing suspension deflection so the MR damper can produce no force – see F_{MR} in the figure 7 b.) during this period.

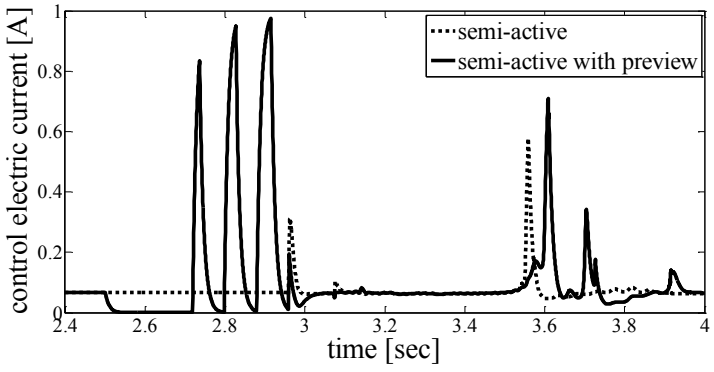

Fig.8: Control electric current flowing through the coil of the MR damper in the quarter car model traveling over a bump controlled with" no preview" and "preview" control strategies

8. Conclusions

The preview controlled active suspension acts the vehicle before the excitation comes, i.e. prepares the vehicle for approaching road disturbances to smoothly travel over them and reduces the probability of undesired tire lift off effect. Active suspension with preview compared with the no preview case provides lower maximum amplitudes and smaller variances of car body acceleration, suspension travel and tire deflection at the same time.

In the case of utilizing the semi-active MR damper in suspension difference between the preview and no preview control strategies almost diminishes. This is because MR damper is only able to dissipate the energy present in the system and cannot generate independent forces when there is no changing suspension deflection.

Acknowledgement

This work was supported by grant Vega 1/0197/12.

References

Hać, A. (1992) Optimal Linear Preview Control of Active Vehicle Suspension. *Vehicle System Dynamics*, 21, pp.167-195.

Hać, A. & Youn, I. (1991) Optimal Semi-Active Suspension with Preview Based on a Quarter Car Model, in*: American Control Conference, 1991*, Boston, MA, USA, pp.433-438.

Havelka, F. & Zuščík, M. & Musil, M. (2010) Návrh spojitého inverzného matematického modelu magnetoreologického tlmiča pre riadenie, in*: Noise and Vibration in Practice: Proceedings of the 15th international acoustic conference, 2010*, Kočovce, Slovensko, pp.53-56.

Hong, S. R. & Choi, S. B. (2005) A hydro-mechanical model for hysteretic damping force prediction of ER damper: experimental verification. *Journal of Sound and Vibration,* 285, pp.1180-1188.

Prabakar, R. S. & Sujatha, C. & Narayanan, S. (2009) Optimal semi-active preview control response of a half car vehicle model with magnetorheological damper. *Journal of Sound and Vibration,* 326, 3-5, pp.400-420.

Thompson, A. G. & Pearce, C. E. M. (1998) Physically Realisable Feedback Controls for a Fully Active Preview Suspension Applied to a Half-Car Model. *Vehicle System Dynamics*, 30, pp.17-35

Úradníček, J. (2008) Multidisciplinárna optimalizácia modelu odpruženia vozidla vybaveného semiaktívnym magnetoreologickým tlmičom. *Kandidátska dizertačná práca*. STU v Bratislave SjF, Bratislava.